

# Optimal Design of Hanging Truss Having SMA Wires (From Vibration Isolation and Attenuation Viewpoints)

Xuan Zhang<sup>1</sup>, Kazuyuki Hanahara<sup>2</sup> & Yukio Tada<sup>1</sup>

<sup>1</sup>Graduate School of System Informatics, Kobe University, Kobe, Japan <sup>2</sup>Faculty of Science and Engineering, Iwate University, Iwate, Japan

Correspondence: Xuan Zhang, Graduate School of System Informatics, Kobe University, Kobe, Japan. E-mail: cs22-tyou@stu.kobe-u.ac.jp

Received: August 23, 2017

Accepted: September 25, 2017

Online Published: November 29, 2017

doi:10.5539/mer.v7n2p53

URL: <https://doi.org/10.5539/mer.v7n2p53>

## Abstract

A column-type truss structure is generally unstable without diagonal bracing members. It is, however, mechanically stable in so-called hanging configuration due to the effect of gravitational force. This kind of structure can isolate an apparatus installed at its tip end from the influence of the vibration of the support ceiling, where the hanging truss structure is placed. The relationship between the stress and strain of the shape memory alloy (SMA) material in relatively high temperature condition has a hysteretic loop, which can be adopted for the purpose of vibration attenuation and isolation. A truss structure with bracing SMA wires in hanging configuration is expected to possess both of the abilities of vibration isolation and attenuation. In this study, optimal placements of SMA wires are obtained by a GA-based approach from the vibration isolation and attenuation points of view under the constraint condition of the number of the SMA wires. Crossover and mutation operators in order to deal with the constraint condition of the number of SMA wire members are proposed. The non-dominated Pareto fronts are obtained for the cases of various numbers of SMA wire members. On the basis of the calculations, it has been confirmed that the number and the placement of the SMA wires are significant factors on the effects of vibration isolation and attenuation. Most of the optimal configurations have one common feature that the SMA wires are distributed close to the middle of the hanging truss structures and there are few SMA wires at the truss units near the support ceiling as well as the peripheral end. The placements of SMA wires in optimal solutions show, however, a tendency of decentralization in the case of emphasis on vibration isolation.

**Keywords:** dynamic behavior, evolutionary algorithm, hanging truss, multi-objective optimization, shape memory alloy wire

## 1. Introduction

In recent years, SMA material has been researched in the area of structural engineering extensively due to the conspicuous characteristics of the shape memory effect and the pseudo-elasticity. The characteristic of pseudo-elasticity demonstrates a hysteretic loop under a specific temperature condition, which can be altered by adjusting the constituents of the material in the process of manufacture. Thus, the composition of the chemical elements is studied and determined on the basis of the working temperature of the SMA material. The hysteretic loop can be utilized for reducing the vibration energy when the SMA material is installed in some type of dynamic structural system. For instance, a multi-linear hysteretic constitutive model of pseudo-elasticity of SMA incorporating residual martensite strain effect has been developed (Parulekar & Reddy, 2012). This model is implemented on a SDOF system and the comparison of the result of experiment and the numerical response has been made. Pseudo-elastic SMA dampers are effective in mitigating the structural response of building structures subjected to strong earthquakes (Qian et al., 2013). The study of Fosdick and Ketema contributes to the understanding of the general macroscopic dynamic characteristics of SMA and its use in vibration damping (Fosdick & Ketema, 1999). Besides, there are studies on vibration isolation using pseudo-elasticity of SMA material (Ghodke & Jangid, 2016; Jose et al., 2017).

Vibration isolation using the characteristics of pendulum type structures has been researched extensively in the recent decades. One of the most significant reasons is that by changing the design parameters of the pendulum type structures, the natural period of the structure can be large enough than the environmental excitation periods; vibration isolation by such kind of structure can be expected. Besides, utilization of some energy absorbing materials contributes to energy attenuation. In the research of Fallah and Zamiri, the genetic algorithm is used to find the optimal values of the isolator (Fallah & Zamiri, 2013). A variable frequency pendulum isolator has been developed (Murnal et al., 2004). The effect of

horizontal and vertical component of seismic load was studied through a kind of pendulum type structure (Jamalzadeh & Barghian, 2015).

In this study, placements of SMA wires in hanging truss are optimally designed using a GA-based method from the viewpoints of vibration isolation and attenuation under the constraint condition of the number of the SMA wires. The evolutionary process of NSGA-based method which contains the elite preservation strategy is demonstrated. In order to reduce the calculation time, a method coupled with the evolutionary optimization algorithm is proposed. The crossover operator and the mutation operator coping with the constraint condition of the number of the SMA wires are proposed. The relationships between the placement of the SMA wire members and the objective functions are discussed. The appropriateness of the proposed optimal calculation algorithm has been confirmed by the simulated examples.

**2. Optimization Problem Dealt with in This Study**

We make a brief introduction on the pseudo-elastic constitutive model of SMA material. Multi-objective optimization formulations are demonstrated and an evolutionary algorithm to deal with the problem is established. The operators for dealing with the constraint condition of the number of the SMA wires are shown.

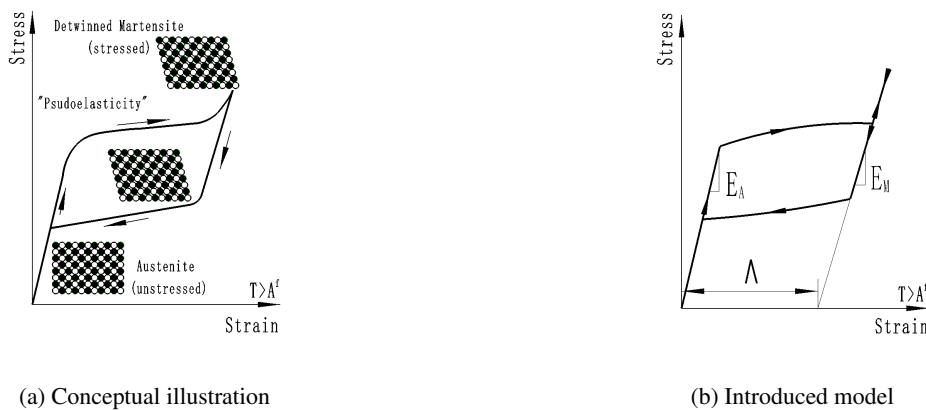


Figure 1. Pseudo-elasticity of SMA

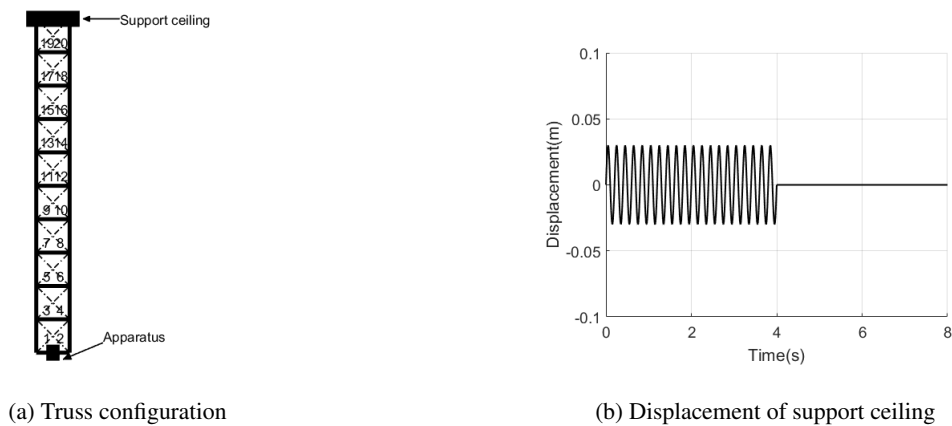


Figure 2. Truss topology (a) and simulated vibration of the support ceiling (b)

**2.1 Constitutive Model of SMA**

Figure 1(a) shows the stress-strain relationship of the pseudo-elastic constitutive model of SMA material considering the crystalline structure of the austenite phase and the martensite phase. For the purpose of simplification of the calculation process, we introduce a piecewise model of pseudo-elasticity as shown in Figure 1(b). The fundamental equations utilized in this research can be seen in (Auricchio & Sacco, 1997; Hu, 2013; Lagoudas et al., 2001).

**2.2 Dynamic Problem**

Dynamic formulations and the corresponding numerical calculation process can be found in (Zhang et al., 2017). The structure dealt with in this study is exhibited in Figure 2(a), where the thick lines stand for rigid members and the broken

lines stand for the possible placements of SMA wire members. In the simulation examples, the environmental motion is given in the form of vibrational motion of the support ceiling, whose corresponding displacement trajectory is sinusoidal shown as the waveform in Figure 2(b). The dynamic behavior in horizontal direction of an apparatus installed at the peripheral end indicated in Figure 2(a) is to be examined.

### 2.3 Formulation of Objective Functions

The objective functions are formulated as the RMS values of the horizontal acceleration of the apparatus assumed at the peripheral end. The vibration isolation and attenuation capabilities are respectively evaluated in terms of the acceleration during and after the vibratory motion of the support ceiling and are expressed as follows:

$$\begin{aligned} W_k &= \left( \frac{1}{T_E} \int_{t=0}^{t=T_E} a_p^2 dt \right)^{(1/2)} \\ V_k &= \left( \frac{1}{T_C} \int_{t=T_E}^{t=T_E+T_C} a_p^2 dt \right)^{(1/2)} \end{aligned} \quad (1)$$

where  $T_E$  is the time period of the vibratory motion of the support ceiling and  $T_C$  is the evaluation time period after the vibration ceased. Subscript  $k$  reflects the number of SMA wires installed in the truss. Parameter  $a_p$  is the acceleration of the apparatus in horizontal direction.

### 2.4 Optimization of the Configuration of SMA Wires

Optimization of the configuration of SMA wires of the truss is dealt with as a combinatorial problem. In order to take account of this multi-objective optimization problem, we deal with the following minimization problem based on the multi-objective function:

$$\begin{aligned} \text{Minimize } F &= F(W_k, V_k) \\ \text{with respect to } &P_{k(1)}, P_{k(2)}, \dots, P_{k(s)}, \dots, P_{k(h_k)} \end{aligned} \quad (2)$$

where  $F$  is the Pareto ranking value of the two objective functions. Pareto ranking describes the relationship of predominance among all of the values in the Pareto solutions and the process for determining the Pareto ranking values is as follows:

- step 1: Set  $r = 1$ .
- step 2: Find all the non-dominated designs. They are referred to as the  $r$ th Pareto front.
- step 3: Eliminate the  $r$ th Pareto front.
- step 4: Repeat from step 2 until all the designs are eliminated, with  $r \leftarrow r + 1$ .

Parameter  $P_{k(s)}$  is the  $s$ th combinatorial pattern of  $k$ -SMA-wire case. Parameter  $h_k$  is the total number of the installation patterns of  $k$  SMA wires. Design variable  $P_{k(s)}$  is expressed in the following binary form as:

$$P_{k(s)} = [b_1 \ b_2 \ \dots \ b_{2u}], \quad b_i = \begin{cases} 0 & \text{(no wire)} \\ 1 & \text{(SMA wire)} \end{cases}$$

Note that the number of '1' bits in  $P_{k(s)}$  is constrained to  $k$ . The bit length  $K$  corresponds to the maximum possible number of SMA wires, where  $K = 2u$  and  $u$  is the number of bays of the truss in the current study.

### 2.5 Optimization Approach

In this research, a NSGA-based multi-objective optimization approach is used (Deb et al., 2002). This approach uses the elite preservation strategy. The constraint condition is the number of the SMA wires. The algorithm is shown as follows:

- step 1: Prepare  $N_{pop}$  individuals as parent population. Generation  $g = 1$ .
- step 2: Evaluate criteria  $W_k$  and  $V_k$ .
- step 3:
  - (1)  $g = 1$ : Determine the rank values.

(2)  $g > 1$ : Select  $N_{pop}$  individuals as parent population in generation  $g$  from the offspring population and the parent population in generation  $g - 1$  based on the order of rank values of the individuals.

step 4: Perform crossover operator and mutation operator to generate the offspring population in generation  $g$ .

step 5: Repeat from step 2 to step 4.

The probability of selection of the  $j$ th individual (Murata et al., 1996) in the process of roulette is expressed as:

$$P_j = \frac{F_j - (F_{max} + 1)}{\sum_{j=1}^{N_{pop}} \{F_j - (F_{max} + 1)\}} \tag{3}$$

where parameter  $F_j$  is the Pareto ranking value of the  $j$ th individual, parameter  $F_{max}$  is the total number of layers of the Pareto fronts which can be attained on the basis of the determination process of the Pareto front ranking as in section 2.4. In order that the rearmost layer of the Pareto front can be selected, we plus 1 to  $F_{max}$  as in Equation (3).

Since we take into account the fixed number of SMA wires of the truss as the constraint condition, the numbers of '1' and '0' bits of the resultant offspring have to be maintained. We introduce the following crossover and mutation operators to cope with the situation. Figure 3 illustrates these operations. The crossover operation shown in Figure 3(a) is as follows:

- step 1: Determine the crossover point randomly in parent 1.
- step 2: Replicate the left part of the crossover point of parent 1 to the left part of the offspring.
- step 3: Cancel the same numbers of 1 and 0 bits of the replicated part from the left part of parent 2.
- step 4: Transfer the rest bits of parent 2 to the right part of the offspring in accordance with the order.

The mutation operation is performed as shown in Figure 3(b) and expressed as:

- step 1: Determine the positions of 1 and 0 of the offspring.
- step 2: Choose a position of 1 and a position of 0 randomly.
- step 3: Change the positions of the selected 1 and 0.

For the purpose of reducing the calculation time of the optimization process, we propose a method for dealing with this situation. All of the individual bit patterns appeared in the course of calculation are recorded along with the corresponding values of the objective functions. Evaluation of the objective functions are performed based on the record in the case that the pattern to be evaluated is already in the record.

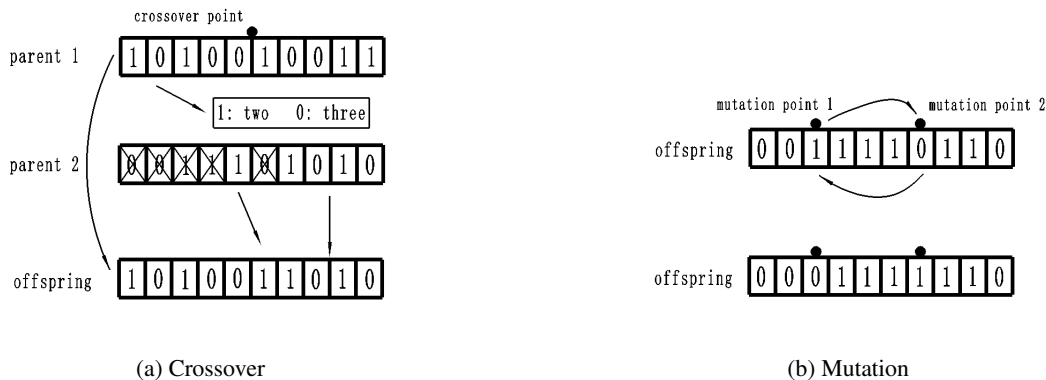


Figure 3. Proposed operators

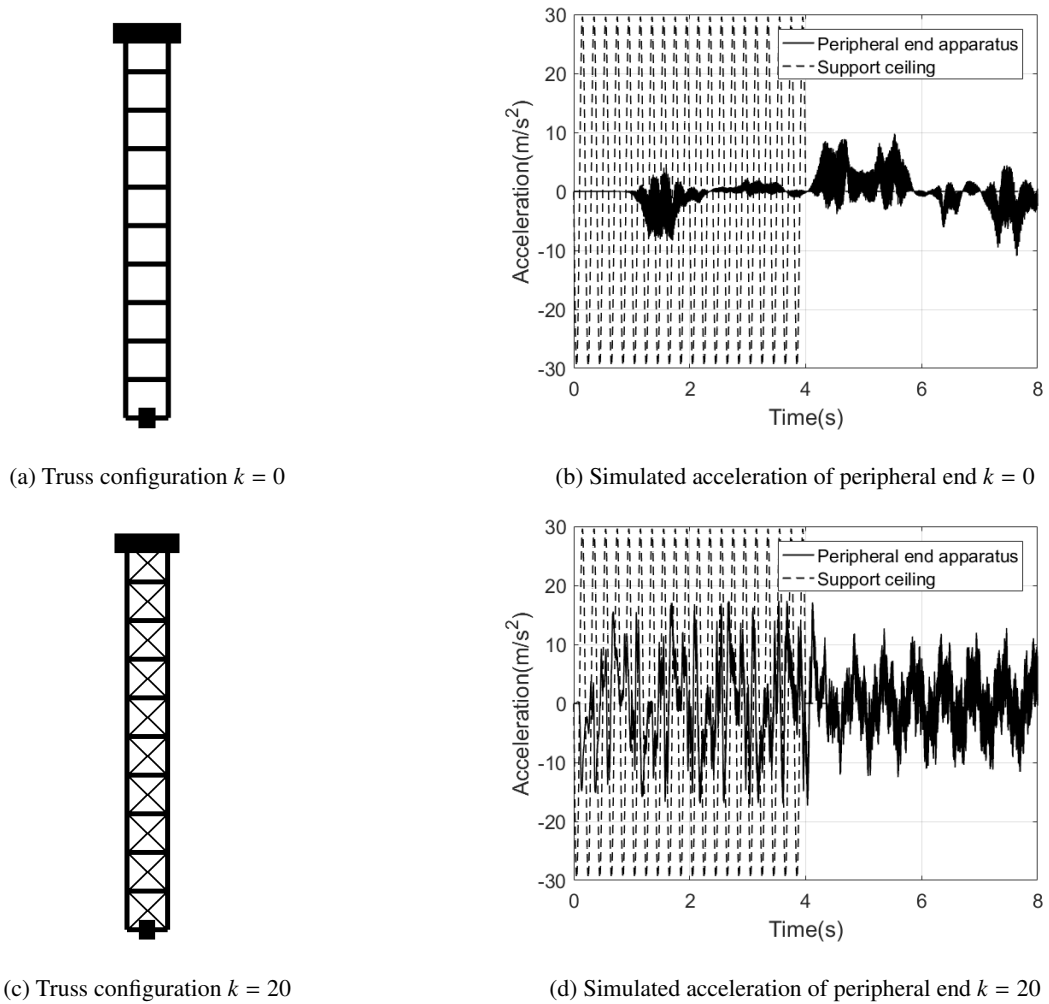


Figure 4. Dynamic behaviors of the hanging truss structures

### 3. Condition of Environmental Vibration and the Typical Behaviors

Table 1. Specification of truss

Parameter	Member	Symbol	Value
Member diameter (mm)	rigid	$a_R$	10mm
	SMA	$a_{sma}$	1mm
Young's modulus (GPa)	rigid	$E_R$	210GPa
Density (kg/m <sup>3</sup> )	rigid	$\rho_R$	7860kg/m <sup>3</sup>
	SMA	$\rho_{sma}$	6500kg/m <sup>3</sup>

Table 2. SMA characteristics

Parameter	Symbol	Value
Maximum phase transformation strain	$\Lambda$	0.05
Young's modulus of austenite phase	$E_A$	70GPa
Young's modulus of martensite phase	$E_M$	30GPa

Typical dynamic behaviors of hanging truss structural system are discussed in order to demonstrate the effects of the hanging configuration and the SMA wire members. Corresponding parameters for the simulations and characteristics of SMA wire are listed in Tables 1 and 2. The vibration frequency of the support ceiling is 5Hz and the amplitude is 0.03m. In our simulation examples, an apparatus of 5kg is assumed to be placed at the peripheral end of the hanging truss for the purpose of suppressing the influence of the vibration of the ceiling. The total mass of the truss without considering the SMA wires and the apparatus is 18.52kg. Time step for the numerical integration is  $50\mu\text{s}$ . This tremendously small time step is for the purpose of dealing with the nonlinearity of this kind of dynamic problem.

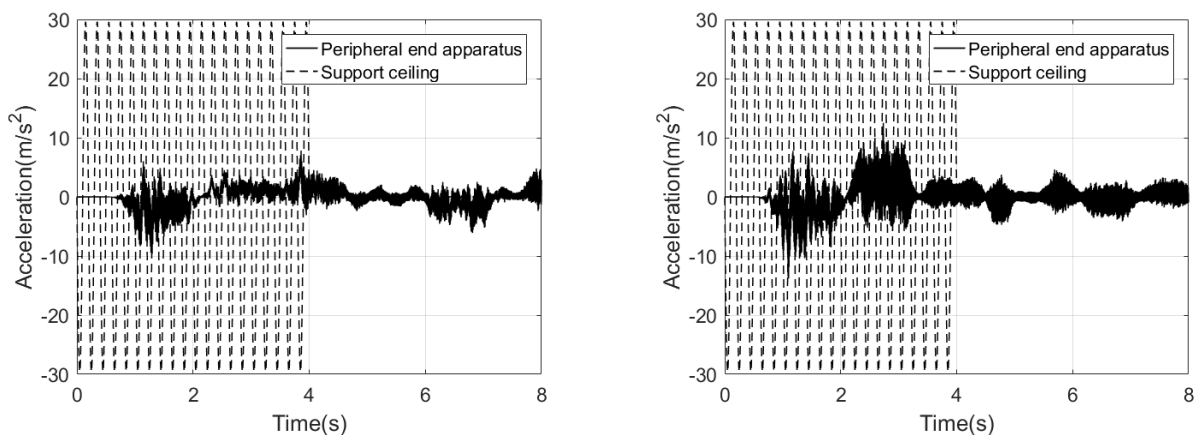
### 3.1 Dynamic Behaviors of the Truss Structures in Typical Configurations

Figure 4(a) is a column-type hanging truss without any bracing wire members ( $k = 0$ ). From the corresponding dynamic behavior result of acceleration in Figure 4(b), we can see the vibration isolation effect in the time period of 0s – 4s. The RMS value in this time period is  $1.60\text{m/s}^2$  and the corresponding value of the support ceiling is  $20.94\text{m/s}^2$ . The vibration isolation is especially obvious at the time period of 0s – 1s due to little vibration energy transmission because there are no bracing wire members and it takes some time to transmit the vibration energy from the support ceiling to the peripheral end. The RMS value at this time period is  $0.05\text{m/s}^2$ .

Figure 4(c) is a hanging truss structure having  $k = 20$  SMA wires. The corresponding acceleration behavior is the result of Figure 4(d). The RMS value of the apparatus acceleration in the time period of 0s – 4s is  $7.72\text{m/s}^2$ . From the two acceleration behaviors shown in Figures 4(b) and 4(d) in the time period of 0s – 4s, we can see that the vibration isolation of truss as shown in Figure 4(a) is more significant. The RMS values of Figures 4(b) and 4(d) in the time period of 4s – 8s are  $2.83\text{m/s}^2$  and  $4.94\text{m/s}^2$  respectively. Therefore, after the cease of vibration motion of the support ceiling, the residual vibration of Figure 4(b) is smaller than that of Figure 4(d). Vibration attenuation effect in Figure 4(d) can be seen. However, owing to the unattenuated vibration energy transmitted from the support ceiling to the peripheral end by the bracing SMA wire members in pure austenite phase, the suppression of residual vibration by attenuation becomes ineffective as can be seen in Figure 4(d), promptly after the vibration of the support ceiling ceased. Because there are no bracing wire members in the truss of Figure 4(a), vibration transmission from the support ceiling to the peripheral end does not occur significantly in this case.

### 3.2 Dynamic Behaviors for Displaying the Vibration Attenuation Capability

Figures 5(a) and 5(b), corresponding to the trusses shown in Figures 7(p) and 7(s), demonstrate typical behaviors of hanging trusses that exhibit both vibration isolation and attenuation capabilities. At the time period of 0s – 4s, the RMS values of Figures 5(a) and 5(b) are  $2.00\text{m/s}^2$  and  $2.94\text{m/s}^2$ , respectively. The RMS values in the time period of 4s – 8s are  $1.35\text{m/s}^2$  and  $1.23\text{m/s}^2$ , respectively. Compare these objective function values with the corresponding function value of Figure 4(b), we can confirm that the vibration isolation of the truss structures in Figures 7(p) and 7(s) are not that excellent but their vibration attenuation capability are better than the truss having no bracing members. This indicates that a hanging truss with a number of bracing pseudo-elastic SMA wires with appropriate configurations have the capability of vibration attenuation.



(a) Behavior of the truss in Figure 7(p) (8-1)

(b) Behavior of the truss in Figure 7(s) (10-1)

Figure 5. Acceleration behaviors of the truss structures for demonstrating vibration attenuation

#### 4. Obtained Optimal Designs

With the constraint condition of the fixed number of bracing SMA wires, the optimal design is conducted by means of the NSGA from the viewpoints of vibration isolation and attenuation. Vibration isolation and attenuation effects are evaluated by the RMS values of acceleration in the time periods of 0s – 4s and 4s – 8s, respectively. The optimal designs for the cases of constraint condition of SMA wires,  $k = 2, 4, 6, 8, 10$  are conducted. In the calculation process, the parameters are as follows for the multi-objective genetic algorithm.

- Population size:  $N_{pop} = 50$ .
- Crossover probability:  $P_{cr} = 0.8$ .
- Mutation probability:  $P_{mu} = 0.01$ .
- Evolution generation:  $g = 100$ .

##### 4.1 Pareto Fronts and Numbers of SMA Wires

Pareto front solutions with the constraint conditions of  $k = 2, 4, 6, 8, 10$  are shown in Figure 6. The abscissa axis is the RMS value in the time period of 4s – 8s, which describes the objective function of vibration attenuation; the ordinate axis is the RMS value in the time period of 0s – 4s, which describes the objective function of vibration isolation. The attached label  $k - c$  denotes the optimized configurations in Figure 7. Label  $c$  means the number of the configuration in the case of  $k$  SMA wires. For example, 10 – 1 is the coordinate of the objective functions of the first optimized configuration with 10 SMA wires that is shown as in Figure 6 and the corresponding truss is shown in Figure 7(s) with the label. For the sake of avoiding untidiness, only the first and the last labels are indicated for each of the Pareto fronts in Figure 6. The solutions listed from the left to the right in the Pareto fronts in Figure 6 with  $k - *$  correspond to the truss configurations from the left to the right in Figure 7 with  $k - *$ , respectively.

We can see that the moving tendency of Pareto front with different values of  $k$  is that the Pareto front moves from the lower right to the upper left in accordance with the increase of the SMA bracing wires. Truss structures in case of small number of SMA wire members show more advantage in vibration isolation and less advantage in vibration attenuation and in case of relatively large number of SMA wire members demonstrate opposite effects.

##### 4.2 Influence of Configurations of SMA Wires

In Figure 6, we can see that the vibration isolation effect when  $k = 0$  is excellent but its vibration attenuation effect is worse than most of other solutions. This demonstrates the capability of vibration attenuation of the bracing SMA wires. However, the solution  $k = 0$  dominates the solution 10 – 8. It means that both of the vibration isolation and vibration attenuation effects for the case of  $k = 0$  is better than the solution 10 – 8. This indicates that an unsuitable placement of SMA wires does not contribute to the vibration attenuation capability even in the case of large number of SMA wires. This is due to the unattenuated vibration energy transmitted from the support ceiling to the peripheral end because of the pure austenite phase of the SMA wires. In addition, the vibration isolation capability due to the pendulum effect of the hanging truss is hindered by the SMA wires in such a case. These conclude that appropriate placement of bracing SMA wires is quite significant for the performance of this truss structure from the viewpoints of vibration isolation and attenuation.

##### 4.3 Influence of Number of SMA Wires

On the basis of the values of criteria given in Figure 6, the optimal designs have better vibration attenuation capability in the case of more SMA wires. In contrast to that, the vibration isolation capability becomes more ineffective in accordance with the number of SMA wires in general. It should be noted, however, that the result of trusses in Figures 7(b) and 7(c) corresponding to the solutions 2 – 2 and 2 – 3 show better performance in both attenuation and isolation capabilities than the truss having no SMA wires.

Even in the case of small number of SMA wires, the residual vibration is destined to be attenuated due to energy absorption by the hysteretic loop of pseudo-elastic SMA wires. Thus, the RMS value of the trusses in Figures 7(b) and 7(c) after the vibration of the support ceiling ceased are smaller than the truss having no SMA wires. The hysteretic loop of the SMA wire also contributes to vibration isolation due to phase transformation strain energy consumption. The vibration transmission due to the bracing SMA wire members is attenuated by the hysteretic loops in the time period of vibration of the support ceiling. The RMS values of these two configurations are smaller than the truss having no SMA wires. The trade-off relationship between the vibration transmission by the bracing members and the energy consumption by the hysteretic loop of the SMA wires can be understood. Suitable number of SMA wires is significant for the performance of the hanging truss against the environmental vibration.

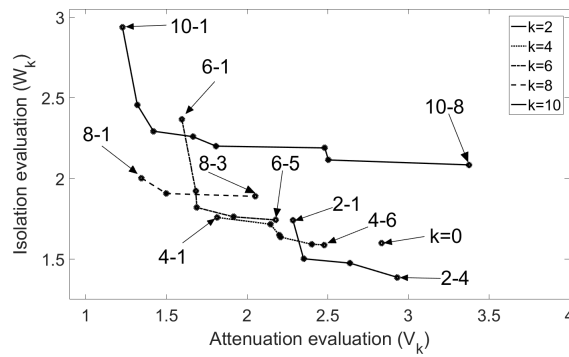


Figure 6. Pareto solutions with the conditions of  $k = 0, 2, 4, 6, 8, 10$

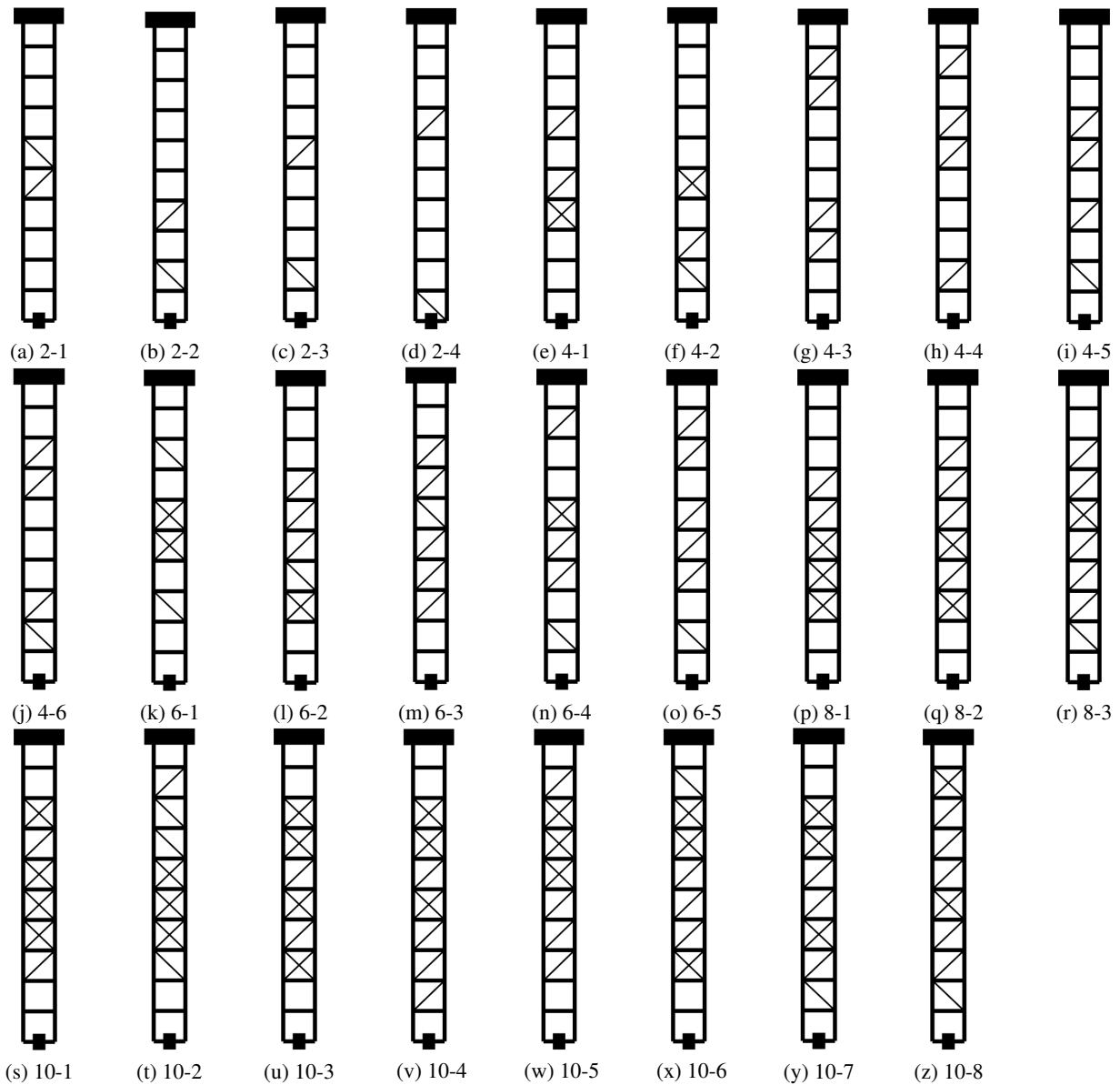


Figure 7. Optimal configurations of the truss

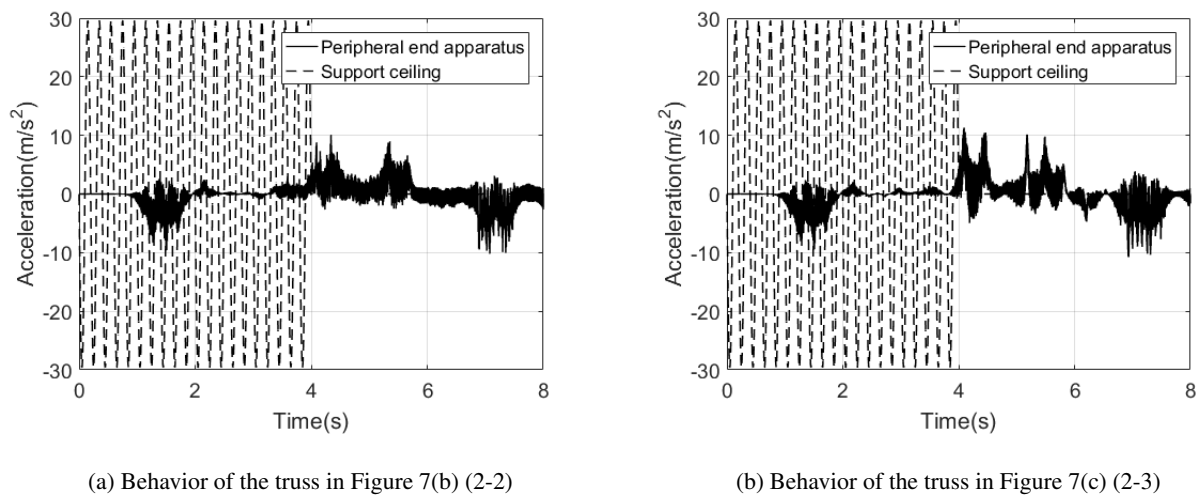


Figure 8. Acceleration behaviors of the truss structures in the case of  $k = 2$

#### 4.4 Overall Tendency of Optimal Configurations

All of these optimal configurations in Figure 7 have two common features. One is that there are no SMA wire members in the truss units which are near the support ceiling or near the apparatus except for the configuration in Figure 7(d). This is a typical feature of structural system for the suppression of vibration transmission from basement to the objective structure by flexible connections at the basement as well as at its peripheral end. The vibration transmission from the ceiling to the truss and from the truss to the peripheral end are suppressed in the case that there are no bracing wire members in the truss unit near the peripheral end as well as the support ceiling. On the basis of this kind of arrangement, the vibration transmission from the support ceiling to the peripheral end can be suppressed due to the effect of pendulum and the energy exerted by the ceiling can be absorbed due to the SMA wire members in the middle truss units simultaneously.

The other common feature is that with an emphasis on vibration isolation, the placement of the SMA wire members becomes approximately more and more decentralized as shown in Figure 7. Owing to the hanging truss structures with ubiquitously distributed placement of the SMA wires, more truss nodes are influenced by the force of the SMA wire members. The residual vibration becomes more significant in such distributions due to more nodes are influenced by the stiff SMA wires in the pure austenite phase. The energy absorption for the attenuation is not sufficient in such cases. On the contrary, in the case of intensively distributed placement of the SMA wires, vibration transmission becomes non-significantly due to less truss nodes are affected by the force of the bracing members and less vibration energy can be transmitted to the peripheral end. Thus, the RMS values of these trusses become smaller relative to the trusses with ubiquitously distributed SMA wires after the vibration of the support ceiling ceased.

In all of these optimal configurations, the number of right-up diagonal SMA wires is significantly larger than the number of right-down diagonal SMA wires. On the basis of the calculations, we noticed that in the time period of 0s-4s, in the cases that the number of the bracing wire members are small, the deformation of the right-up SMA wire is significantly larger than the deformation of the right-down SMA wires. More hysteretic loop can be utilized to consume the vibration energy in such configurations that the number of right-up diagonals is larger than the right-down diagonals.

Most of these optimal configurations demonstrate better vibration attenuation effects than the hanging truss having no bracing members since no energy consumption members are in the hanging truss without SMA wire members. A few number of the optimal configurations with larger RMS values than the hanging truss having no SMA wires after the vibration of the ceiling ceased. The reason is that the vibration is transmitted by those bracing SMA wire members to the peripheral end; however, those transmitted vibration energy can not be totally attenuated due to the pure austenite phase of those SMA wire members after the vibration of the support ceiling ceased.

## 5. Conclusion

In this study, we studied a truss structure having the capabilities of vibration isolation and attenuation. The isolation effect is achieved by the hanging configuration of a column-type truss structure which demonstrates the characteristic of pendulum; the attenuation effect is achieved by the pseudo-elastic mechanical property of SMA wire members which demonstrates a hysteretic loop of the relationship between stress and strain. Once the topology of the hanging truss is fixed, there are two factors influence the dynamic behaviors of the structure: the number and the configuration of SMA

wire members.

In the case that relatively large number of SMA wire members are placed at the hanging truss, the characteristic of pendulum is less evident. Therefore, the number of the SMA wires is a significant factor on the vibration isolation effect. Inappropriate placements of the SMA wires also lead to insufficient effect from the vibration reduction point of view. Taking both of these two factors into consideration, we conducted an optimization problem of this hanging truss from vibration isolation and attenuation viewpoints under the constraint condition of the number of SMA wire. The algorithm of a non-dominated sorting genetic algorithm in order to deal with this multi-objective optimization problem is constructed. The operators for the purpose of coping with the constraint condition has been developed.

On the basis of the calculations, we obtained that most of the optimal configurations have one common feature that the SMA wires are placed significantly in the middle part of the optimally designed trusses. The placements of SMA wires in optimal solutions show a tendency of decentralization in the case of emphasis on vibration isolation.

## References

- Auricchio, F., & Sacco, E. (1997). A One-Dimensional Model for Superelastic Shape-Memory Alloys with Different Elastic Properties between Austenite and Martensite. *International Journal of Non-linear Mechanics*, 32(6), 1101-1114. [https://doi.org/10.1016/S0020-7462\(96\)00130-8](https://doi.org/10.1016/S0020-7462(96)00130-8)
- Deb, K., Pratap, A., Agarwal, S., & Meyarivan, T. (2002). A Fast and Elitist Multiobjective Genetic Algorithm: NSGA-II. *IEEE transactions on evolutionary computation*, 6(2), 182-197. <https://doi.org/10.1109/4235.996017>
- Fallah, N., & Zamiri, G. (2013). Multi-Objective Optimal Design of Sliding Base Isolation Using Genetic Algorithm. *Scientia Iranica*, 20(1), 87-96. <https://doi.org/10.1016/j.scient.2012.11.004>
- Fosdick, R., & Ketema, Y. (1998). Shape Memory Alloys for Passive Vibration Damping. *Journal of Intelligent Material Systems and Structures*, 9(10), 854-870. <https://doi.org/10.1177/1045389X9800901009>
- Ghodke, S., & Jangid, R. S. (2017). Influence of High Austenite Stiffness of Shape Memory Alloy on the Response of Base-Isolated Benchmark Building. *Structural Control and Health Monitoring*, 24(2). <https://doi.org/10.1002/stc.1867>
- Hanahara, K., Zhang, X., & Tada, Y. (2016). Dynamic Simulation of Adaptive Truss Consisting of Various Types of Truss Members. *Mechanical Engineering Research*, 6(1), 75-87. <https://doi.org/10.5539/mer.v6n1p75>
- Hu, J. W. (2013). Numerical Simulation for the Behavior of Superelastic Shape Memory Alloys. *Journal of Mechanics Science and Technology*, 27(2), 381-386. <https://doi.org/10.1007/s12206-012-1268-8>
- Jamalzadeh, A., & Barghian, M. (2015). Dynamic Response of a Pendulum Isolator System under Vertical and Horizontal Earthquake Excitation. *Periodica Polytechnica. Civil Engineering*, 59(3), 433. <https://doi.org/10.3311/PPci.7848>
- Jose, S., Chakraborty, G., & Bhattacharyya, R. (2017). Coupled Thermo-Mechanical Analysis of a Vibration Isolator Made of Shape Memory Alloy. *International Journal of Solids and Structures*, 115, 87-103. <https://doi.org/10.1016/j.ijsolstr.2017.03.001>
- Lagoudas, D. C., Mayes, J. J., & Khan, M. M. (2001). Simplified Shape Memory Alloy (SMA) Material Model for Vibration Isolation. *Smart Structures and Materials 2001: Modeling, Signal Processing, and Control in Smart Structures*. <https://doi.org/10.1117/12.436514>
- Murata, T., Ishibuchi, H., & Tanaka, H. (1996). Multi-Objective Genetic Algorithm and Its Applications to Flowshop Scheduling. *Computers and Industrial Engineering*, 30(4), 957-968. [https://doi.org/10.1016/0360-8352\(96\)00045-9](https://doi.org/10.1016/0360-8352(96)00045-9)
- Murnal, P., & Sinha, R. (2004). Aseismic Design of Structure-Equipment Systems Using Variable Frequency Pendulum Isolator. *Nuclear Engineering and Design*, 231(2), 129-139. <https://doi.org/10.1016/j.nucengdes.2004.03.009>
- Parulekar, Y. M., & Reddy, G. R. (2011). Nonlinear Model of Pseudoelastic Shape Memory Alloy Damper Considering Residual Martensite Strain Effect. *Advances in Acoustics and Vibration*, vol. 2012, Article ID 261896, 11 pages. <https://doi.org/10.1155/2012/261896>
- Qian, H., Li, H. N., Song, G. B., & Guo, W. (2013). Recentring Shape Memory Alloy Passive Damper for Structural Vibration Control. *Mathematical Problems in Engineering*, 2013, Article ID 963530, 13 pages. <https://doi.org/10.1155/2013/963530>
- Zhang, X., Hanahara, K., & Tada, Y. (2017). Dynamic Characteristics of Hanging Truss Having Shape Memory Alloy Wires. *Mechanical Engineering Research*. In printed.

**Copyrights**

Copyright for this article is retained by the author(s), with first publication rights granted to the journal.

This is an open-access article distributed under the terms and conditions of the Creative Commons Attribution license (<http://creativecommons.org/licenses/by/4.0/>).